9th International IEEE EMBS Conference on Neural Engineering
San Francisco, CA, USA, March 20 - 23 , 2019

Transfer learning using low-dimensional subspaces for EMG-based classification of hand posture

Sezen Yağmur Günay[1], Mathew Yarossi[1,2], Dana H Brooks[1], Eugene Tunik[2], Deniz Erdoğmuş[1]

***Abstract*— This study proposes a novel approach for evaluating the task invariance of muscle synergies, vital for potential implementation in improving prosthetic hand control. We do this by using a transfer learning paradigm to test for invariance across a relatively small set of hand/forearm muscle synergies, derived from electromyographic (EMG) activation patterns during voluntary behaviors such as finger spelling and grasp mimicking postures and unconstrained exploration. EMG for each task were decomposed using non-negative matrix factorization into synergy and weight matrices, and cross-task weights for each task were then reconstructed by employing the base matrices from different tasks. Support Vector Machine and Extreme Learning Machine classifiers were used to classify the resulting weights in order to compare their performance, as well as their behaviors as a function of synergy rank. Both algorithms showed robust and significantly higher performance, compared to two distinct randomized controls, with lower rank EMG representations, both within and between tasks/postures, supporting hypotheses of functional invariance of multi-muscle synergies. Our results suggest that this invariance could be leveraged to efficiently calibrate postures for prosthetic hand implementation by transferring learned EMG patterns from unconstrained movements to other tasks.**

I. Introduction

Availability of dexterous upper limb prostheses that intuitively respond to a users intention is an ambitious goal that could dramatically improve the lives of millions worldwide. Recording surface electromyography (EMG) provides access to a user's voluntary neuromuscular drive and can be used to myoelectrically control a powered prostheses. However, despite decades of research, most commercially available devices utilize a simple two muscle, binary-based controller to actuate a simple hand posture (i.e., open vs close [1]). Development of more dexterous multifunctional myoelectric control requires pattern classification of multi-muscle EMG to derive movement intent [2]. To this end, evidence that the complexity of human voluntary control may be reduced via identifying multi-muscle patterns with a fixed relative balance of activation that act as "modules", commonly referred to as muscle synergies, has received substantial attention in the myoelectric powered prostheses community [3], [4]. It has been suggested that accurate capture of these low dimensional control features could offer potential advantages over single muscle direct drive, including reduced control complexity, lower sensitivity to amplitude cancellations, and greater robustness to slight shifts in electrode position [5], as well as offer a richer set of prosthetic movement options. Gesture classification from EMG muscle synergies has been successfully implemented for task-dependent problems [6], [7], [5]. However, the gap between the synergy assumption and practical cross-task implementation remains an open area of investigation. Key to bridging this gap is testing the extent to which synergies transfer across tasks and postures, as well as finding a reliable methodology to classify labeled postures from synergy representations. We address these two open problems using a machine learning approach.

Several machine learning methods, including artificial neural networks (ANN), linear discriminant analysis (LDA), support vector machines (SVM), and Gaussian mixture models have been previously used in myoelectric-based motion control using EMG data, with variable but generally favorable accuracy. To the best of our knowledge, the only methods previously applied specifically to synergy-based gesture classification are SVMs [8] and a variant of ANN's called Extreme Learning Machines (ELMs) [7]. However as noted above, they have only been tested in settings where the low dimensional structure of muscle activations was derived from the same data set that was used for gesture classification. Here we investigate the ability to *transfer* synergy patterns across three different task domains, as described below. We compare SVM vs. ELM classifiers for this purpose and report on the sensitivity of ELM to the particular set of random initialization weights.

II. Methodology

A. Data Collection

Five healthy, right-handed, subjects (4 males; mean age 25.6 $\pm$ 3.2) participated after providing institutionally approved informed consent. Subjects were seated comfortably with the elbow supported and wrist free to move. Surface EMG (Delsys Inc. Trigno, Natick, MA, USA) was recorded at 2kHz from the 16 lower arm muscles shown in Fig. 1.

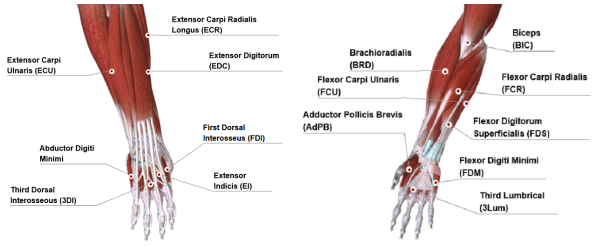

(a) Posterior View (b) Anterior View

Fig. 1. Visualization of muscles targeted during experiment.

[1]SYG, MY, DHB and DE are with SPIRAL Group, Department of Electrical and Computer Engineering, Northeastern University, Boston, MA 02115, USA {gunay, brooks, erdogmus}@ece.neu.edu

[2]MY and ET are with the Department of Physical Therapy, Movement and Rehabilitation Science, Northeastern University, Boston, MA 02115, USA {m.yarossi, e.tunik}@northeastern.edu

978-1-5386-7921-0/19/$31.00 ©2019 IEEE

Each participant performed the following three tasks:

- American Sign Language (ASL): All subjects were naïve to American Sign Language prior to participation. Subjects shaped their right hand into letters and numbers of the ASL posture set (Fig. 2(a)) presented as pictures on a computer screen (33 postures, 3x/posture, 99 trials). Dynamic letters 'J' and 'Z' were omitted, along with the number '0', which is visually the same as the letter 'O'.
- Grasp Mimicking (GM): Subjects mimicked 13 grasps and an open palm position (Fig. 2(b)), presented as pictures on a computer screen (14 postures, 3x/posture, 84 trials).
- Unconstrained Movement (Free): Subjects were instructed to take 2 minutes to freely explore the movement space with their fingers, hand, and wrist, avoiding maintaining any specific posture for more than 1 second (3x, 6 minutes total).

For ASL and GM tasks, participants were given 2 seconds to form the posture, 6 seconds to maintain it, and 2 seconds to rest between trials. Participants were instructed to form each character or grasp with force sufficient to form and maintain the posture as if they were signing to someone or holding the depicted item, respectively. Participants were instructed to limit motion at the elbow during the experiment.

(a) ASL (modified from [6]) (b) Grasp Mimicking

Fig. 2. ASL (a) and Grasp (b) postures presented to subjects

B. Preprocessing and Feature Extraction

EMG data were filtered offline with 5-th order Butterworth band-pass (0.1 Hz to 400 Hz) and 60 Hz notch filters using custom written software (Matlab, Mathworks). For ASL and GM tasks, only data from the 6 second "posture maintenance" potion of each trial were used for further analysis. Given the instructions for maintaining the posture (constant-force, constant-angle, non-fatiguing contraction), we assumed steady muscle activity. In [9], it has been mathematically and experimentally shown that EMG amplitude can be statistically represented using the root mean square (RMS), given assumptions of stationarity and Gaussianity. We note that if the distribution is Laplacian, maximum likelihood estimates of the EMG amplitude would be obtained using the mean absolute value (MAV) of the time series signal. However our prior work confirmed that RMS yielded higher classification accuracy [10], implying a Gaussian distribution, so we employed RMS as the principled approach in the current study. For the ASL and GM tasks, where we had stationary epochs, the 6 second-long EMG time series of each posture was cut into non-overlapping 300 ms epochs, with 100 ms data between the above epochs eliminated as buffer periods. This yielded 15 sample epochs per trial. For the free movement task, which clearly was not stationary, the entire 2 minute time series was cut into 300 ms epochs. The RMS value for each 300 ms epoch was calculated and submitted to further analysis.

The basic assumption in previous work on muscle synergies is that there are underlying groupings of muscles with fixed relative activation strengths, and that EMG activity can be described as a linear weighted sum of these groupings. In this model, both the synergies bases and activation weights are intrinsically non-negative. Identifying muscle synergies that sufficiently explain the aggregate EMG activity can be considered mathematically as a dimensionality reduction problem, and solved under the non-negativity constraint. For this reason, non-negative matrix factorization (NMF) is widely used for synergy analysis. The input to the NMF algorithm is a muscle by time ($C \times T_1$) matrix X and the factorized outputs are a base matrix W of size C×R where R≤C and an activation matrix H which is $R \times T_1$.

Two different feature extraction techniques were implemented in this study. The first was an inter-class classification, in which we selected one of three datasets as the basis data ($X_{base} \in \mathbb{R}^{C \times T_1}$) and applied NMF to extract the base ($W_{base} \in \mathbb{R}^{C \times R}$) and activation matrices ($H_{activation} \in \mathbb{R}^{R \times T_1}$) such that:

$$X_{base} \approx W_{base} H_{activation} \tag{1}$$

The bases obtained from this analysis were used to estimate activation weights from one of the other tasks ($X_{est} \in \mathbb{R}^{C \times T_2}$) using a non-negative least squares (NNLS) algorithm so as to satisfy the non-negativity constraint (see (2)). We note that for classification purposes, the free movement data does not have labels and thus cannot be classified, so we used that data only for obtaining base matrices but not for obtaining activation weights. We also note that we differentiate between T_1 and T_2 since the number of epoch samples differs across the three different types of activity.

$$\begin{aligned} \underset{W,H}{\text{minimize}} \quad & \frac{1}{2}||X_{est} - W_{base}\tilde{H}_{est}||_F^2 \\ \text{subject to} \quad & \tilde{H}_{est} \geq 0 \end{aligned} \tag{2}$$

In the second technique, intra-class classification, we derived synergy bases in order to classify data obtained from the same task. For this part of the work, which can be considered as a control analysis to compare to the results of inter-class technique, we used a slightly different feature extraction technique. In order to diversify data selection, one group of data were randomly split into 10-folds. Equation (1) was applied across 9 training folds and then H_{est} was calculated over the 10^{th} fold ((2)). Again, this approach was only applicable for the grasp mimicking and ASL datasets since Free movement data did not have labels.

C. Gesture Classification

SVM: We employed a nonlinear, one-vs-one SVM classifier with a radial basis function kernel to evaluate the

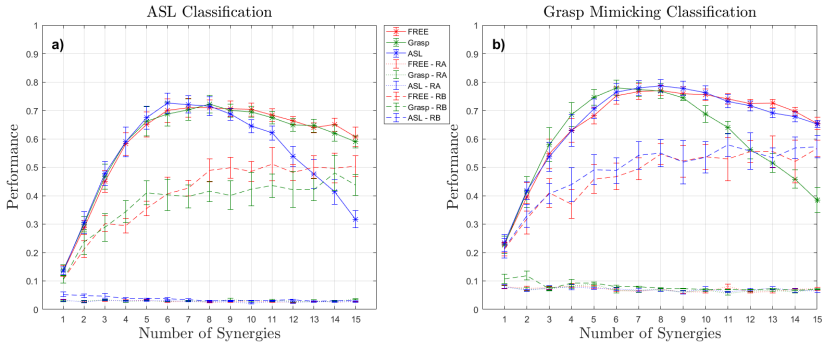

Fig. 3. SVM classification results as a function of the number of synergies estimated (rank). In each panel the solid, dashed and dotted lines represent classification using actual synergies and activations (both estimated from data), using activations estimated from random bases (RB) scaled to match the real bases, and using random activations (RA) scaled to match the real activations, respectively (see text for details). In panel (a) we show results for classification of ASL data, and in panel (b) for classification of the grasp mimicking data. The first word listed in the legend, along with the color, identifies the task from which bases and activations were estimated, and the second word, along with the line type, identifies whether bases and activations were estimated from data or randomized using the RA or RB methods. In panel (a) the intra-class classification is given in blue, whereas, all other colors are inter-class decoding results. Similarly, the intra-class results are represented in green in panel (b) and other colors represent inter-class results. Error bars show standard error of the mean.

transferred information learned from different datasets. Since all $t \in T_2$ columns of H_{est} had a specific label, this matrix was randomly divided into ten groups. At each step, the model was trained on nine groups and tested on the last group. The validation performance measure was defined as the probability of correct classification; this was estimated by averaging results over the 10 folds. Selection of the base matrix rank ($R \in \{1,\ldots,15\}$) is an important model order selection issue; here we used the validation performance measure estimate, in a process in which each classification problem was exhaustively repeated for all 15 possible values of R.

To evaluate classification performance using the estimated bases and activations, we compared to randomized bases and activations, employing two different randomization techniques. First, we evaluated the element-wise mean and variance of the H_{est} matrices used for each classifier and then replaced them by random matrices with independent entries generated from a Gaussian distribution with the same mean and variance. This comparison condition is referred to below as random activation (RA) classification. Second, mean and variance calculations were applied to the W_{base} matrices calculated from the data to generate random *base* matrices with matching element-wise means and variances. NNLS was then used to calculate H_{est} for classification. We refer to this condition as random base (RB) classification. Another dimensionality reduction technique was not employed for bench marking, since it has been shown that NMF outperforms principal component analysis [10].

ELM: We carried out the same classification tasks using ELMs. The number of hidden layer neurons was selected as 150 and a sigmoid function was employed as the non-linear activation function. Since ELMs have an additional level of variability due to their use of random weights in their first layer, in addition to using the same 10-fold cross-validation process described above, for each fold we trained 10 separate ELMs with different draws of randomized first layer weights, in order to assess the sensitivity of ELM performance to this random effect.

III. Results

A. Classification Results

In order to evaluate predictability, base matrices evaluated on all three datasets were used to calculate the activation matrices of the labelled datasets (ASL and GM). The group mean SVM classification performance as a function of number of synergies (rank) for 10 fold-cross validation for actual data as well as RA and RB chance level conditions (see Sec. II-C) are shown in Fig. 3. Panel (a) of Fig. 3 illustrates how the classification accuracy changed for the ASL data prediction problem as the rank of the base matrix increased from one to fifteen while Fig. 3(b) shows the corresponding results on the grasp mimicking data. A two-way repeated measures ANOVA with factors DataType (Real, Random Bases) and Rank (1-15) was used to evaluate if classification performance was significantly different from chance. Significant interactions were followed with pairwise t-test with Bonferroni correction for multiple comparisons ($p = .05/15 = .0033$) to determine if classification accuracy calculated from measured data was significantly different from RB data for each rank. For classification of ASL postures, DataType X Rank interactions were significant when the bases were derived from ASL ($F(14,149)=23.61$, $p<.001$), GM ($F(14,149)=6.45$, $p<.001$), and Free ($F(14,149)=6.52$, $p<.001$). Post-hoc pairwise t-test indicated significant differences between real data and RB data for ranks (ASL, [1-15]; GM [7,8,9,11,13]; Free [4,5,7,10,12]). Classification of grasp postures found that their DataType X Rank interactions were significant when the bases were derived from ASL ($F(14,149)=2.65$, $p=.002$), GM ($F(14,149)=20.71$, $p<.001$), and Free ($F(14,149)=2.73$, $p=.002$). Post-hoc pairwise t-test indicated significant differences between real data and RB data for ranks (ASL, [6]; GM [2-15]; Free [6,7,8]).

Since the number of possible classes for ASL classification was higher than that of the grasp mimicking task, it is not surprising that accuracy was lower for ASL classification. We also observed that any rank (number of synergies) between $5-7$ yielded the highest performance for both problems. Fur-

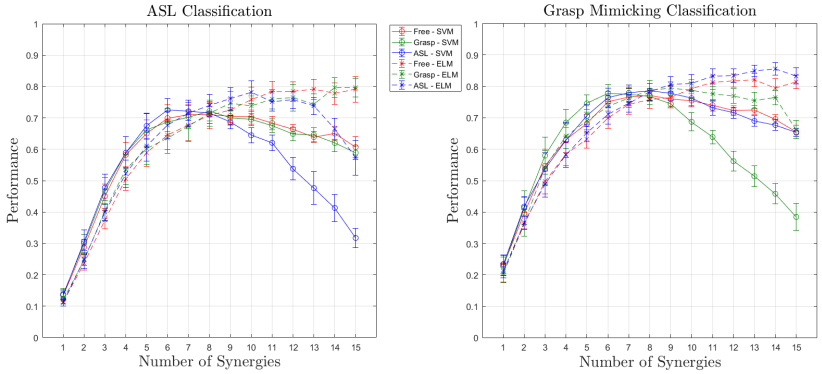

Fig. 4. Results from ELM classifier compared to SVM results for both classification tasks. SVM curves (dotted) are repeated from Fig 3. ELM curves follow the same format but using dashed lines. Error bars show standard errors across subjects.

thermore, the effect of over-fitting with higher rank was more dramatic when classifying a task from its own data (when the base matrix and the estimation activation weights were calculated on the same data). Overall, results d that when SVM was used for classification, derivation of synergies from a different dataset than the target of classification not only yielded comparable accuracy to the within-classification condition but was also more resistant to over-fitting. Perhaps most importantly, we found that a low-dimensional structure of muscle activation derived from an unlabeled/unconstrained task (here, free movement) could possibly be used to reduce the long daily calibration time necessary for prosthetic hand applications when utilized for gesture classification.

Comparison between SVM and ELM classifier results are shown in Fig. 4. SVM curves are repeated from Fig. 3 for ease of comparison. ELM performance is lower than SVM for small ranks (below 7), but higher at larger ranks, as SVM seems to suffer from overfitting more than ELM, whose performance declines only at ranks above 12 for same-task classification and not at all for cross-task classification. This suggests that the tradeoff between low-dimensionality and classification accuracy is classifier dependent and must be treated carefully. The SVM architecture seemed to make better use of the low dimensional nature of synergies, and therefore may be more suited to a synergy based classifier. In contrast, ELM performed best at full-rank, perhaps because neural networks inherently exploit information abundance.

Our study of the sensitivity of the ELM algorithm to random weight initialization found that its effect on classification performances was negligible ($\sim$100 times lower than the lowest classification accuracy), indicating ELM performance was robust to the random weight initialization.

IV. Conclusion

We developed a transfer learning scheme utilizing muscle synergies across different classification tasks, and compared the performance of two popular classifiers for this purpose. Direct comparisons of classification performance results evaluated on the data collected from 5 subjects during ASL, grasp mimicking and unconstrained hand gesture sessions revealed that NMF derived synergies were functionally task-invariant. Cumulatively, our results indicate that an unconstrained data collection session, even of a short duration, may be possible for prosthetic hand controller calibration for implementation across other untrained functional tasks. We speculate that the muscle synergy classification problem is ripe for investigation using newer classifiers, which might improve on SVM performance while obtaining better low-rank performance than ELM.

Acknowledgment

Our work is supported by NSF IIS-1149570 (DE), CNS-1544895 (DE), CBET-1804550 (ET, DE, DB), NIH R01DC009834 (DE), R01NS085122 (ET), and 2R01HD058301 (ET).

References

[1] B. Waryck, "Comparison of two myoelectric multi-articulating prosthetic hands." Myoelectric Symposium, 2011.

[2] M. Hakonen, H. Piitulainen, and A. Visala, "Current state of digital signal processing in myoelectric interfaces and related applications," *Biomedical Signal Processing and Control*, vol. 18, pp. 334–359, 2015.

[3] G. C. Matrone, C. Cipriani, M. C. Carrozza, and G. Magenes, "Real-time myoelectric control of a multi-fingered hand prosthesis using principal components analysis," *Journal of Neuroengineering and Rehabilitation*, vol. 9, no. 1, p. 40, 2012.

[4] S. Godfrey, A. Ajoudani, M. Catalano, G. Grioli, and A. Bicchi, "A synergy-driven approach to a myoelectric hand," in *Rehabilitation Robotics (ICORR), 2013 IEEE International Conference on*. IEEE, 2013, pp. 1–6.

[5] S. Muceli, N. Jiang, and D. Farina, "Extracting signals robust to electrode number and shift for online simultaneous and proportional myoelectric control by factorization algorithms," *IEEE Transactions on Neural Systems and Rehabilitation Engineering*, vol. 22, no. 3, pp. 623–633, 2014.

[6] A. Ajiboye and R. Weir, "Muscle synergies as a predictive framework for the EMG patterns of new hand postures," *Journal of Neural Engineering*, vol. 6, no. 3, p. 036004, 2009.

[7] C. W. Antuvan, F. Bisio, F. Marini, S.-C. Yen, E. Cambria, and L. Masia, "Role of muscle synergies in real-time classification of upper limb motions using extreme learning machines," *JNAR*, vol. 13, no. 1, p. 76, 2016.

[8] J. A. Suykens and J. Vandewalle, "Least squares support vector machine classifiers," *Neural Processing Letters*, vol. 9, no. 3, pp. 293–300, 1999.

[9] N. Hogan and R. W. Mann, "Myoelectric signal processing: Optimal estimation applied to electromyography-part i: Derivation of the optimal myoprocessor," *IEEE Trans. on Biomedical Engineering*, no. 7, pp. 382–395, 1980.

[10] S. Y. Günay, F. Quivira, and D. Erdoğmuş, "Muscle synergy-based grasp classification for robotic hand prosthetics," in *Proceedings of the 10th International Conference on PErvasive Technologies Related to Assistive Environments*. ACM, 2017, pp. 335–338.